Multi-Δt approach for peak-locking error correction and uncertainty quantification in PIV

Adatrao, Sagar; Sciacchitano, Andrea

Multi-Δt approach for peak-locking error correction and uncertainty quantification in PIV

Sagar Adatrao* and Andrea Sciacchitano

Department of Aerospace Engineering, Delft University of Technology, Delft, The Netherlands

*s.adatrao@tudelft.nl

Abstract

A novel approach is devised for the quantification of the systematic uncertainty due to peak locking in particle image velocimetry (PIV), which also leads to correction of the peak-locking errors. The approach relies on a linear regression of the measured displacements from multiple Δt acquisitions (Δt being the time separation between two frames of an image pair). In presence of peak locking, the measured particle image displacement is not a linear function of Δt as the measurement error varies non-linearly with the sub-pixel particle image displacement. In the proposed approach, image acquisition is conducted with multiple Δt's, and then a linear regression is carried out among the measured time-averaged displacements at different Δt's, yielding a regression displacement. When the Δt's are selected properly, the latter represents a correction to the measured displacement where systematic errors due to peak locking are significantly diminished. The expression of the standard uncertainty in the regression displacement is provided. The regression displacement (and velocity) can also be used to quantify the systematic uncertainty due to peak locking in the measured time-averaged displacements (and velocities). The methodology is first assessed with synthetic data and then applied to planar PIV experiments on a uniform flow and an airfoil wake flow. Reference measurements with much larger Δt than the Δt's of the actual measurements (such that relative peak-locking errors are negligible for the former) are used to validate the proposed approach in both the experiments. Uncertainty coverages for the estimated uncertainties in the velocities measured in the experiments of the uniform flow and the wake flow are of 67% and 59%, respectively, which are comparable to 68% confidence level at which the uncertainties are computed. This proves the validity of the proposed multi-Δt approach for peak-locking uncertainty quantification.

1 Introduction

Peak locking (also referred to as pixel locking) is recognized as one of the major error sources in PIV measurements. Such an error source, mainly ascribed to particle image diameters small with respect to the sensor's pixel size, causes a bias of the measured particle image displacement towards the closest integer value (Westerweel 1997, Adrian and Westerweel 2011, Michaelis et al. 2016, Raffel et al. 2018). It is particularly relevant in high-speed PIV measurements with CMOS cameras, whose large pixel size (of the order of 10 to 20 μm) yields particle image diameters often smaller than one pixel. Thus, the recent development of high-speed cameras has been influencing the study on peak-locking errors and their correction in PIV. Also, the peak-locking errors significantly affect the turbulence statistics extracted from the PIV measurements (Christensen 2004) which is another motivation for quantification and correction of the peak-locking errors.

Several approaches have been proposed for quantification and correction of the peak-locking errors. A-priori estimations and correction of the peak-locking errors based on theoretical models were presented by Angele and Muhammad-Klingmann (2005) and Cholemari (2007). Both the models have showed the effect of peak locking on the turbulence statistics following the work of Christensen (2004). The peak-locking errors have been corrected by assuming Gaussian distribution for the displacement and velocity probability density functions in the former model

(Angele and Muhammad-Klingmann 2005), whereas the correction has been achieved by assuming sinusoidal variation of the peak-locking error with respect to the sub-pixel displacement in the latter model (Cholemari 2007). A number of works on the peak-locking correction at the processing (i.e. velocity estimation) and post-processing stages have been devised in the literature. Roth and Katz (2001) have applied a histogram equalization to the sub-pixel particle image displacements for the correction. However, Hearst and Ganapathisubramani (2015) have demonstrated that pixel locking is non-uniform across an image. Therefore, identifying and adjusting for pixel locking with histograms computed based on the entire vector fields, as done by Roth and Katz (2001), may have been erroneous and the equalization process should be applied on a vector-by-vector basis (Hearst and Ganapathisubramani 2015). However, their approach is effective only in the absence of other error sources as they might affect the histogram of the measured displacements and velocities. The peak-locking errors arising at the processing stage can be reduced by using state-of-the-art processing algorithms. However, the peak-locking errors due to small particle image diameters are difficult to resolve. The concept of defocusing to increase the particle image diameter has been a common practice and a slight defocusing has been effective in reducing the peak-locking errors as reported by Overmars et al. (2010). However, the optimal amount of defocusing is not possible to estimate and the excessive defocusing increases random errors in the detection of the particle images. Furthermore, defocusing cannot be applied in tomographic measurements, which otherwise increase the number of ghost particles due to the lack of the focus and in turn the uncertainty in the results. An optical diffuser (Michaelis et al. 2016) can solve these issues in which larger particle image diameters have been obtained by increasing a point spread function of the imaging system. The reduction of both systematic and random error components of the measured velocity by a factor of 3 was achieved by Kislaya and Sciacchitano (2018). However, the effectiveness of the diffusers is limited for the CMOS cameras with large pixel size. A spread of about 10 μm for the incoming light can be achieved on the image plane using the diffusers (Michaelis et al. 2016). However, it is smaller than the pixel size of the CMOS cameras (20 μm) required for high-speed measurements.

The discussion above shows that the problem of peak locking errors due to small particle image diameters, especially in the case of CMOS cameras for high-speed PIV measurements, is still unsolved. In such a situation, a continuous development in the approaches based on multiple Δt image acquisition (Nogueira et al. 2009, Nogueira et al. 2011, Legrand et al. 2012, Legrand et al. 2018) has shown a high potential in peak-locking error quantification and correction, Δt being a time separation between two frames in PIV. Using a set of different Δt's for the same flow measurement allows for segregating the errors that scale with Δt (e.g. peak-locking errors) from the errors that do not (Nogueira et al. 2011). For the case of an unknown turbulent flow and an unknown measurement uncertainty, multiple particle image displacements measured at multiple Δt acquisitions can be used to estimate a turbulence level of the wind tunnels (Scharnowski et al. 2019). The recent work of Legrand et al. (2018) has offered a 1-D analytical modeling of the peak-locking errors and has allowed for measurement correction. However, the method is iterative and computationally expensive to estimate calibration coefficients mentioned in the algorithm. Also, selection of two Δt's is not trivial in presence of turbulence in the flow and Δt values should be adjusted for different levels of turbulence. In the present work, a simple approach based on linear regression of the measured displacements from multiple Δt acquisitions is proposed to correct the peak-locking errors and quantify the uncertainty in the measured displacement. The proposed methodology is explained in Section 2 with the help of synthetically generated data. It is then assessed for two planar PIV experiments with a uniform flow and a wake flow of an airfoil in a wind tunnel, the results of which are presented in Section 3.

2   Proposed methodology

To explain the proposed methodology for peak-locking errors correction and uncertainty quantification, consider the case of a flow measurement where the local actual time-averaged

velocity is u_{true}, constant in time. When PIV measurements are conducted with inter-frame time separation Δt, the actual time-averaged particle image displacement (not affected by any measurement error is):

$$\Delta x_{true} = u_{true} \cdot \Delta t \tag{1}$$

From equation (1) it is evident that the actual particle image displacement increases linearly with the inter-frame time separation. In presence of the peak-locking errors, the measured particle image displacement is the sum of the true displacement and the measurement error. The peak-locking errors are often modelled as a sinusoidal (or close-to-sinusoidal, Cholemari 2007) function of the sub-pixel particle image displacements, hence they vary non-linearly with Δx_{true}. Therefore, the measured particle image displacement becomes a non-linear function of Δt. If the measurements are repeated with multiple Δt's, performing a linear regression of the measured displacements yields a regression displacement $\Delta x_{reg}(\Delta t)$ which is a better estimate of Δx_{true} (see Figure 1).

2.1 Quantification of peak-locking uncertainty

Total uncertainty in the measured time-averaged displacement at each Δt can be expressed by:

$$U_{\overline{\Delta x}}\left(\Delta t\right) = \sqrt{U^2_{b\left(\overline{\Delta x}\right)} + U^2_{b,corr\left(\overline{\Delta x}\right)}\left(\Delta t\right) + U^2_{p\left(\overline{\Delta x}\right)}\left(\Delta t\right)} \tag{2}$$

where, $U_b(\overline{\Delta x})$, $U_{b,corr}(\overline{\Delta x})$ and $U_p(\overline{\Delta x})$ are systematic uncertainty, correlated systematic uncertainty and precision uncertainty in the time-averaged displacement ($\overline{\Delta x}$), respectively.

The systematic uncertainty can be estimated with respect to the displacement obtained from the regression:

$$U_{b\left(\overline{\Delta x}\right)} = t_{C.I.,\nu}\sqrt{\frac{1}{n-2}\sum_{i=1}^{n}\left[\overline{\Delta x}\left(\Delta t_i\right) - \Delta x_{regr}\left(\Delta t_i\right)\right]^2} \tag{3}$$
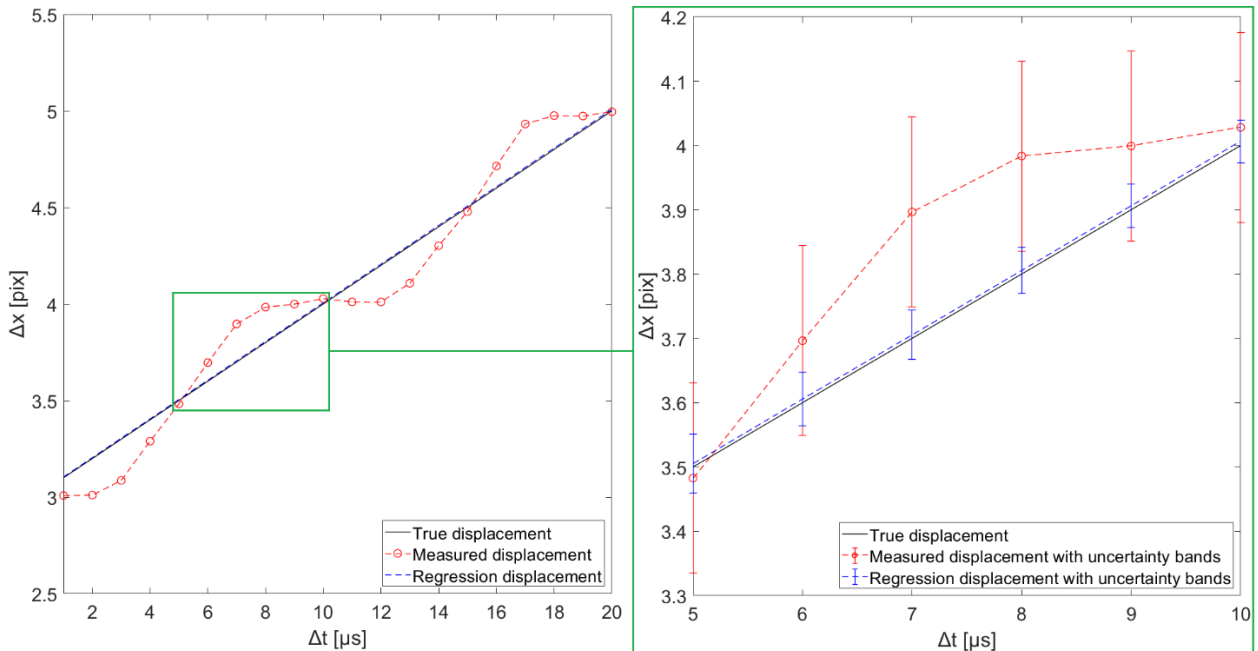

Figure 1: Plots of true displacement, measured displacements and regression displacements with uncertainty bands for multiple Δt acquisitions in the synthetic data

where, $t_{C.I.,v}$ is the t-statistic describing the desired confidence interval and n is the number of Δt acquisitions. This systematic uncertainty due to peak locking constitutes major part of the total uncertainty in the mean displacement.

The correlated systematic uncertainty is also included in equation (2) considering the fact that the instantaneous measured displacements might be correlated in PIV experiments and is expressed as follows using Taylor's approach of uncertainty propagation (Coleman and Steele 2009):

$$U^2_{b,corr(\overline{\Delta x})}(\Delta t) = 2\sum_{i=1}^{N-1}\sum_{j=i+1}^{N}\left(\frac{\partial \overline{\Delta x}}{\partial \Delta x_i}\right)\left(\frac{\partial \overline{\Delta x}}{\partial \Delta x_j}\right)\sigma^2_{\varepsilon_b(\Delta x_i),\varepsilon_b(\Delta x_j)} \qquad (4)$$

where, N is the number of instantaneous measured displacements (Δx) at each Δt acquisition. The equation (4) is further simplified considering that the covariance between the bias errors in the successive instantaneous displacements can be replaced by the product of correlation coefficient (ρ) between them and the individual standard deviations (σ) assuming normal distribution for the bias errors (ε_b).

$$U^2_{b,corr(\overline{\Delta x})}(\Delta t) = \frac{2}{N^2}\sum_{i=1}^{N-1}\sum_{j=i+1}^{N}\rho_{\varepsilon_b(\Delta x_i),\varepsilon_b(\Delta x_j)}\cdot\sigma_{\varepsilon_b(\Delta x_i)}\cdot\sigma_{\varepsilon_b(\Delta x_j)} \qquad (5)$$

The estimation of the correlated systematic uncertainty $[U_{b,corr}(\overline{\Delta x})]$ is complex as the bias errors in the instantaneous displacements are unknown and difficult to determine. Also $U_{b,corr}(\overline{\Delta x})$ is negligible in the case of statistically resolved measurements, as is the case in the present work. Hence, it can be neglected while calculating the total uncertainty using equation (2).

The third term under the radical in equation (2) represents the random (precision) uncertainty due to the finite number of samples (Coleman and Steele 2009) and is given by:

$$U_{p(\overline{\Delta x})}(\Delta t) = \frac{t_{C.I.,v}}{\sqrt{N}}\sqrt{\frac{1}{N-1}\sum_{i=1}^{N}\left[\Delta x_i(\Delta t)-\overline{\Delta x}(\Delta t)\right]^2} \qquad (6)$$

The total uncertainty in the measured time-averaged velocity ($\overline{u}$) at each Δt acquisition can then be estimated using Taylor's approach from the uncertainty in the time-averaged displacement [calculated using equation (2)] at that particular Δt acquisition:

$$U_{\overline{u}}(\Delta t) = \frac{U_{\overline{\Delta x}}(\Delta t)}{\Delta t} \qquad (7)$$

The total uncertainties in the measured mean displacements and velocities at different Δt acquisitions estimated in the synthetic data are shown in Fig. 1 and Fig. 2, respectively. It is to be noted that the uncertainties in the displacement and velocity along the X-axis are calculated and shown. However, the same equations can be used to calculate the uncertainties in the displacement and velocity along the other directions. The uncertainties in the measured displacements are around 0.15 pixels at different Δt's and around 0.3 to 0.5 m/s in the measured velocities. It is observed that the uncertainty in the measured velocity decreases with the increasing Δt (or Δx) as the relative peak-locking errors for larger displacements (at larger Δt's) are less than those for the smaller displacements (at smaller Δt's), as also reported by Kislaya and Sciacchitano (2018). This fact is used in the experiment (explained in section 3 of this paper) in which reference measurements are carried out with a much larger Δt than the actual measurement Δt's and the proposed approach of uncertainty quantification is then validated by comparing the actual measurements with the reference ones.
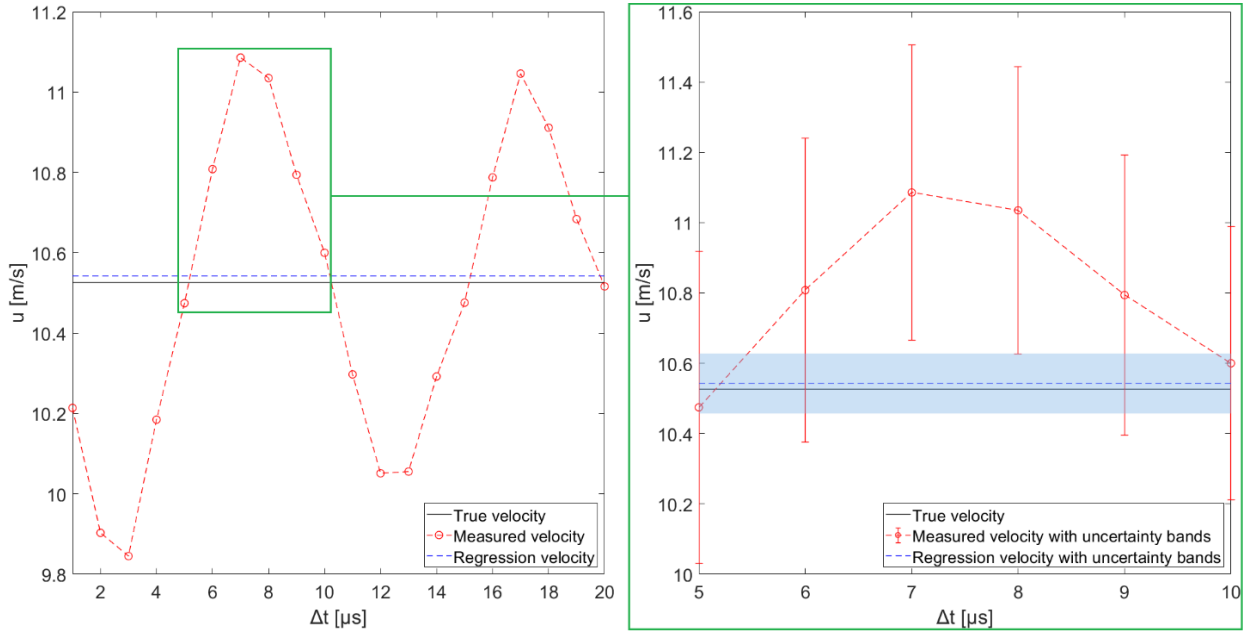
Figure 2: Plots of true velocity, measured velocities for multiple Δt acquisitions and regression velocity with uncertainty bands in the synthetic data

2.2 Correction of peak-locking errors

The peak-locking errors in the time-averaged PIV measurements can be corrected for by correcting the bias errors. Thus, the measured displacements and velocities ($\overline{\Delta x}$ and $\overline{u}$) are replaced with the displacements and velocity from regression (Δx_{regr} and u_{regr}), respectively. The total standard uncertainty in the corrected displacement at each Δt acquisition is then given by the uncertainty of the regression model (Coleman and Steele 2009):

$$U_{\Delta x_{regr}}\left(\Delta t\right) = U_{b\left(\overline{\Delta x}\right)}\sqrt{\frac{1}{n} + \frac{\left(\Delta t - \overline{\Delta t}\right)^2}{\sigma_{\Delta t,\Delta t}}} \tag{8}$$

where, $U_{b\left(\overline{\Delta x}\right)}$ is the systematic peak-locking uncertainty in the measured mean displacement [calculated using equation (3)], n is the number of Δt's and $\sigma_{\Delta t,\Delta t}$ is the covariance in the Δt's:

$$\sigma_{\Delta t,\Delta t} = \sum_{i=1}^{n}\Delta t_i^2 - \frac{\left(\sum_{i=1}^{n}\Delta t_i\right)^2}{n} \tag{9}$$

The uncertainty in the corrected velocity is then derived from the uncertainty in the corrected displacement using Taylor's approach. It is to be noted that the uncertainty in the velocity is calculated at mean of Δt's and uncertainty in the corresponding displacement from the regression. The choice of mean of Δt's is based on the fact that the mean value of independent data points (Δt's in our case) shows the best estimated value for the dependent variable (Δx in our case) where the regression error is the least (Montgomery et al. 2001).

$$U_{u_{regr}} = \frac{U_{\Delta x_{regr}}\left(\overline{\Delta t}\right)}{\overline{\Delta t}} \tag{10}$$

where, $\overline{\Delta t}$ is the mean of Δt's. The equation (10) can further be simplified by referring the equation (8):

$$U_{u_{regr}} = \frac{1}{\sqrt{n}} \left[\frac{U_{b(\overline{\Delta x})}}{\overline{\Delta t}} \right] \tag{11}$$

The uncertainty bands calculated using equations (8) and (11) for the corrected displacements and velocity are shown in Fig. 1 and Fig. 2, respectively, for the synthetic data. The uncertainties in the corrected displacements (Δx_{regr}) are around 0.03 to 0.06 pixels at different Δt's and 0.09 m/s for the corrected velocity (u_{regr}). Thus, the uncertainties in the measured displacements and velocities are reduced by 57 to 78% and 73 to 83%, respectively, after correction with the displacements and velocity from regression, respectively. These differences in the uncertainties in the uncorrected (measured) and corrected (from regression) displacements and velocities are clearly visible in the zoomed-in plots in Fig. 1 and Fig. 2, respectively.

3 Experimental assessment

The multi-Δt approach for uncertainty quantification is assessed with two planar PIV experiments on a uniform flow and a wake flow of NACA0012 wing at 15 degrees angle of attack.

3.1 Experimental setup and procedure

The experiments are conducted at the W-tunnel of Delft University of Technology, which is an open-jet open-return wind tunnel with an exit cross section of 40 × 40 cm² and an area contraction ratio of 9. The maximum achievable free-stream velocity is 30 m/s with 0.3% turbulence intensity (Tummers 1999). In this experiment, the free stream velocity is set to 10 m/s. The flow is seeded with micron-sized water-glycol droplets produced by a SAFEX seeding generator. A LaVision High Speed Star 6 CMOS camera (12 bits, 20 μm pixel size, 1024 × 1024 pixels) and a Quantronix Darwin-Duo (Nd:YLF, 25 mJ pulse energy at 1 kHz, 527 nm wavelength) are used for the measurements. The camera mounts a Nikon objective lens of 105 mm focal length, and the optical aperture is set to $f^{\#}$ = 8 and $f^{\#}$ = 5.6 for the experiments of the uniform flow and wake flow, respectively. The sensor size is cropped to 512 × 512 pixels and 1024 × 640 pixels for the uniform flow and wake flow measurements, respectively, resulting in field of views (FOV) of 53 mm × 53 mm and 134 mm × 84 mm, respectively, as shown in Fig. 3. The particle image diameters of 0.6 pixels and 0.4 pixels are achieved with magnification factors of 0.19 and 0.15 in the uniform flow and wake flow experiments, respectively, following the formulation presented by Raffel et al. (2018). The small particle image diameters cause peak locking in the measured displacements. In both the experiments, image acquisition is conducted at a frequency of 200 Hz with multiple Δt's from 10 μs to 30 μs in steps of 1 μs. For each Δt the time-averaged displacement is measured at each spatial location in the image via the LaVision DaVis 8.4 software, using Gaussian interrogation windows of 128 × 128 pixels with 75% overlap for the initial passes and 16 × 16 pixels with 75% overlap for the final passes. The proposed methodology (explained in section 2 of this paper) is applied to estimate the corrected displacements and velocity using regression analysis. The approach is also validated using reference measurements for both the experiments. Following Kislaya and Sciacchitano (2018), the reference measurements are conducted with a time separation Δt_{aux} (488 μs for the uniform flow and 196 μs for the wake flow) which is much larger than the Δt's (10-30 μs) used in the actual measurements. Due to the large displacement (Δx_{aux}) in the reference measurements, the relative peak-locking error in Δx_{aux} is negligible with respect to that in the measured displacements at Δt's. The reference displacement (Δx_{ref}) at each Δt is thus calculated from the auxiliary displacement (Δx_{aux}) measured at Δt_{aux}:
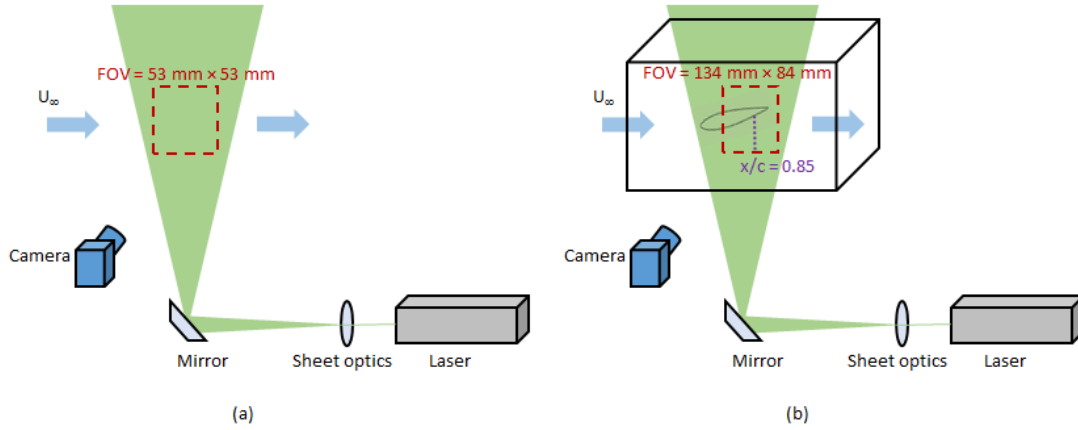
Figure 3: Schematic experimental setup for (a) uniform flow and (b) wake flow of NACA0012 wing at 15 degrees angle of attack

$$\Delta x_{ref} = \Delta x_{aux} \frac{\Delta t}{\Delta t_{aux}} \tag{12}$$

and the reference velocity is equal to the auxiliary velocity from the reference measurements:

$$u_{ref} = u_{aux} \tag{13}$$

The errors in the measured displacements and velocities at each Δt can then be calculated with respect to the reference displacements and reference velocity, respectively:

$$\varepsilon_{\overline{\Delta x}}(\Delta t) = \overline{\Delta x}(\Delta t) - \Delta x_{ref}(\Delta t) \tag{14}$$

$$\varepsilon_{\overline{u}}(\Delta t) = \overline{u}(\Delta t) - u_{ref} \tag{15}$$

These errors in the measured displacements and velocities are used to estimate the reliability of the uncertainty approach. The uncertainty coverages are calculated for the uncertainties in the measured displacements and velocities calculated using equations (2) and (7), respectively. An uncertainty coverage is the percentage of measurements for which the errors are contained within the uncertainty limits (Timmins et al. 2012):

$$\left| \varepsilon_{\overline{\Delta x}}(\Delta t) \right| \le U_{\overline{\Delta x}}(\Delta t) \tag{16}$$

$$\left| \varepsilon_{\overline{u}}(\Delta t) \right| \le U_{\overline{u}}(\Delta t) \tag{17}$$

The uncertainty coverage should be equal to the confidence level at which the uncertainty is evaluated (68% in the present work). The uncertainty estimation is thus more accurate if the uncertainty coverage is closer to 68%.

3.2 Results

The results of the application of the proposed methodology to the uniform flow experiment are summarized in Fig. 4 and Fig. 5. From the displacement plots of Fig. 4, it is evident that the reference displacement increases linearly with the inter-frame time separation, whereas the measured displacement exhibits an oscillatory behavior which is consistent with the presence of peak-locking errors (Cholemari, 2007). In fact, sub-pixel displacements between 0 and 0.5 pixels yield under-estimated displacement measurements, whereas fractional displacements between 0.5 and 1 pixels

yield over-estimated displacement measurements. The errors are approximately null at fractional displacements of 0 and 0.5 pixels. The regression displacement curve is much closer to the reference displacement, indicating a significant reduction in peak-locking errors. The uncertainty bands are also shown for both the uncorrected (measured) and corrected displacements (from regression) in zoomed-in plot in Fig. 4. The uncertainties in the measured displacements are reduced by 58 to 78% when correcting the measured displacements by linear regression. The uncertainties in the measured displacements are around 0.1 pixels at different Δt's, whereas those on the regression displacements are around 0.02 to 0.04 pixels.
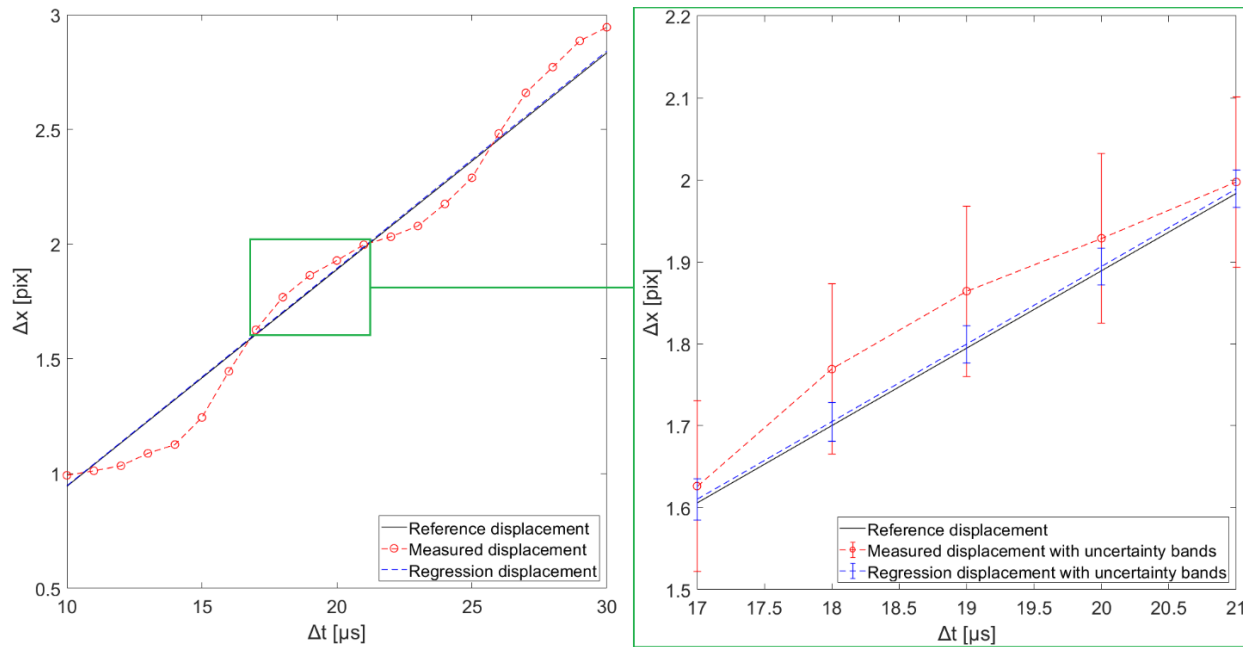

Figure 4: Plots of reference displacement, measured displacements and regression displacements with uncertainty bands for multiple Δt acquisitions in the uniform flow experiment
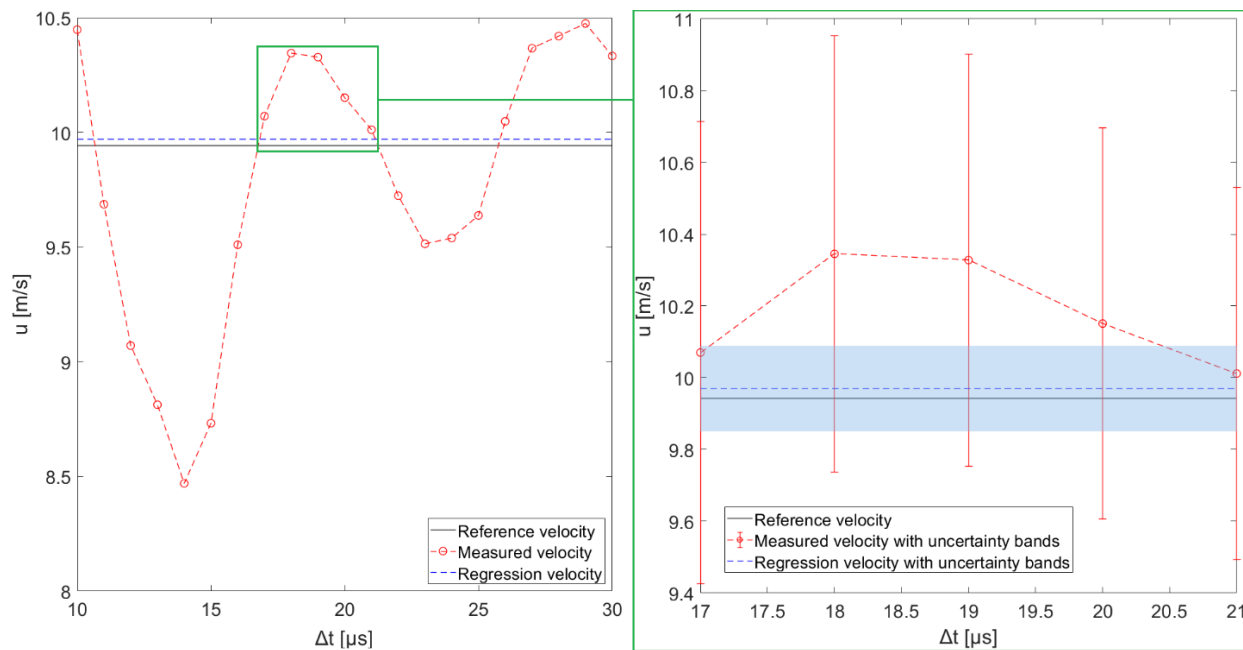

Figure 5: Plots of reference velocity, measured velocities for multiple Δt acquisitions and regression velocity with uncertainty bands in the uniform flow experiment

Analogous results in terms of velocity are illustrated in Fig. 5. The uncertainty in the corrected velocity estimated from the regression analysis is 0.12 m/s, which is much smaller than the uncertainties in the measured velocities (0.36 to 1.09 m/s) at different Δt's. The uncertainty coverages for the uncertainties in the measured displacements and velocities are also calculated following equations (16) and (17), respectively, for the uniform flow experiment. The uncertainties exhibit a coverage of 67% considering the measurements at different Δt acquisitions, which is comparable to the desired coverage of 68%. The analysis, thus, proves the validity of the multi-Δt approach for uncertainty quantification.

The proposed methodology is also applied to the experiment of wake flow where the mean velocity field estimated in the reference measurement can be seen in Fig. 6. The results are plotted in Fig. 7 for the spatial points along a vertical dotted line at 85% of the chord as shown in Fig. 3(b) and Fig. 6. The vertical position in space is represented by y/c which is equal to zero at the surface of the wing and increases in the downward direction away from the surface. Fig. 7 shows the velocities from the reference measurement, measured velocities at Δt's equal to 10 µs and 14 µs (velocities at only two Δt's are shown for sake of clarity), and the regression velocities estimated from the regression analysis (considering the measured displacements at all Δt's from 10 µs to 30 µs). The results are shown in zoomed-in plots for three regions- I, II, III which represent the regions in wake, shear layer and free stream, respectively. The first major observation is that the time-averaged velocities are over-estimated in the measurements with 10 µs, whereas they are under-estimated with 14 µs of time separation. Although these two Δt's are comparable to each other, a clear systematic shift is observed in the velocities due to the peak locking. The second major observation is that the peak-locking errors are the largest in the free-stream region (III), where fluctuations in the flow are negligible and cannot suppress the significant peak-locking errors in that region, whereas they are lower in the turbulent wake, which is consistent with the findings of Christensen (2004). The uncertainties in the measured velocities are around 0.19 to 1.13 m/s and 0.13 to 0.80 m/s in the measurements with 10 µs and 14 µs of time separations, respectively, whereas those of the corrected velocities estimated from the regression (u_{regr}) are around 0.02 to 0.12 m/s along the vertical dotted line shown in Fig. 6. The uncertainties in the measured velocities are reduced by 90% and 86% in the measurements with Δt's equal to 10 µs and 14 µs, respectively, after correction with the velocities from regression as can be seen in the zoomed-in plots in Fig. 7. The uncertainties in the measured velocities exhibit a coverage of 59 % considering the measurements at different Δt acquisitions at the spatial locations along the vertical dotted line shown in Fig. 3(b) and Fig. 6.
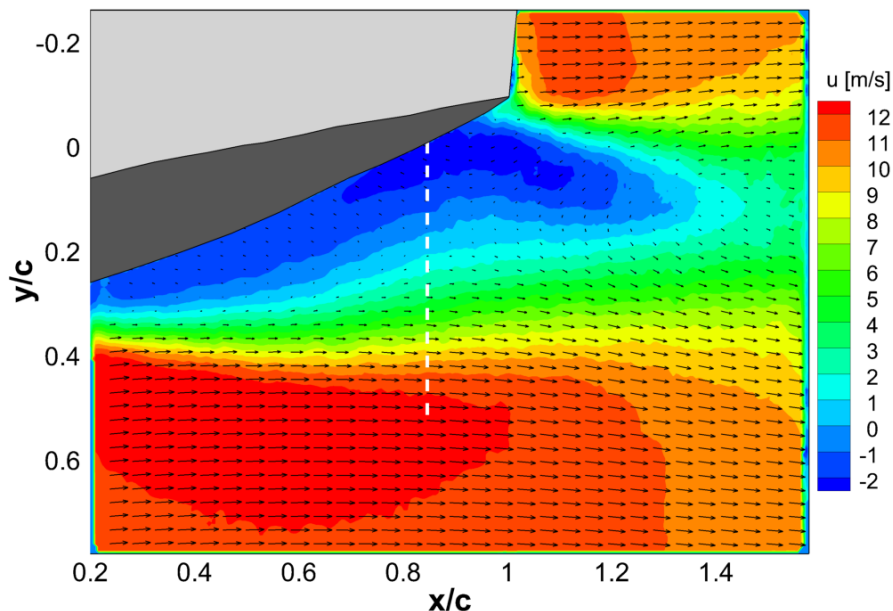

Figure 6: Mean velocity field estimated in the reference measurement in the wake flow experiment
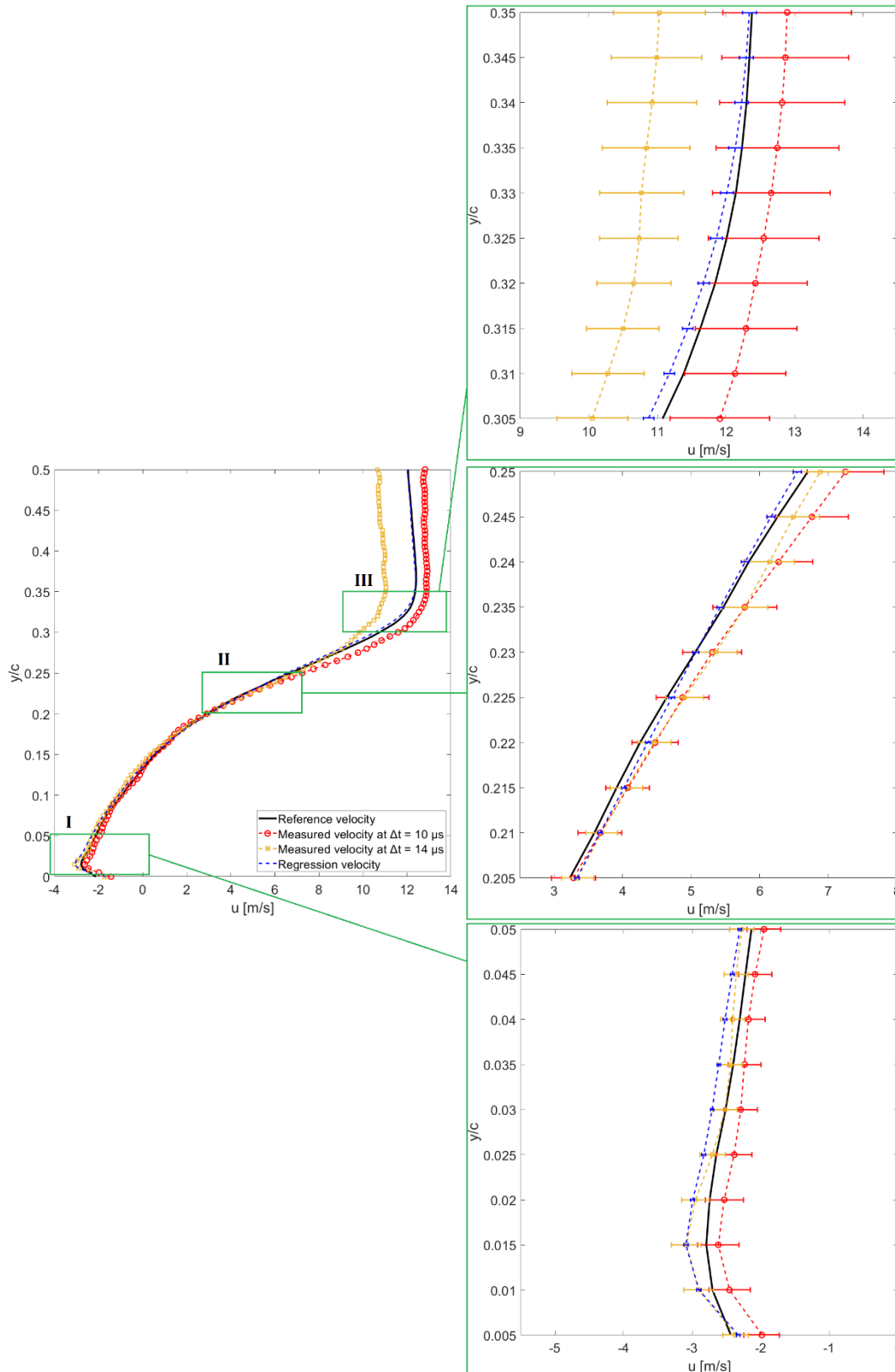
Figure 7: Plots of reference velocities, measured velocities at Δ*t* equal to 10 μs and 14 μs, and regression velocities with uncertainty bands in the wake flow experiment [The velocities are plotted at *x/c* = 0.85, where *y/c* = 0 at the surface of the wing and increases in the downward direction away from the surface as shown by a vertical dotted line in Fig. 3(b) and Fig. 6]

4 Conclusions

A novel approach is proposed for the quantification of the peak-locking systematic uncertainty in PIV, which in turn also corrects the measured particle image displacement and velocity for peak-locking errors. The theoretical framework of the methodology described, and its performances are assessed via synthetic data as well as planar PIV experiments on a uniform flow and a wake flow of an airfoil. The approach is based on the assumption that local flow statistics is constant in time, according to which the particle image displacement should vary linearly with the time separation (Δt) between two frames. However, in presence of peak locking, the measured particle image displacement is a non-linear function of Δt as the measurement error in the displacement varies non-linearly with sub-pixel particle image displacement. The approach thus relies on a linear regression of the measured displacements from multiple Δt acquisitions, where the displacement and velocity from the regression analysis can be used to quantify systematic errors and uncertainty due to peak locking in the measured displacement and velocity, respectively. Furthermore, the displacement and velocity from regression represent a more accurate estimate of the "true" values. The methodology is assessed for planar PIV experiments of the uniform flow and the wake flow using reference measurements with much larger Δt than the measurement Δt's. The uncertainty coverages comparable to 68% confidence level are observed in both the experiments which proves the validity of the approach. The present work introduces and outlines the approach for peak-locking uncertainty quantification and correction. The investigation thus estimates the systematic peak-locking uncertainty in the measured particle image displacement and velocity. Future research will focus on extending the methodology for uncertainty quantification of higher order statistics (Reynolds normal and shear stresses).

Acknowledgements

References

Adrian RJ and Westerweel J (2011) *Particle Image Velocimetry*. Cambridge University Press, Cambridge, United Kingdom

Angele KP and Muhammad-Klingmann B (2005) A simple model for the effect of peak-locking on the accuracy of boundary layer turbulence statistics in digital PIV. *Experiments in Fluids* 38:341-347

Cholemari MR (2007) Modeling and correction of peak-locking in digital PIV. *Experiments in Fluids* 42:913-922

Christensen KT (2004) The influence of peak-locking errors on turbulence statistics computed from PIV ensembles. *Experiments in Fluids* 36:484-497

Coleman HW and Steele WG (2009) *Experimentation, Validation, and Uncertainty Analysis for Engineers*. John Wiley and Sons Inc., Hoboken, N.J., 3rd edition

Hearst RJ and Ganapathisubramani B (2015) Quantification and adjustment of pixel-locking in particle image velocimetry. *Experiments in Fluids* 56:191

Kislaya A and Sciacchitano A (2018) Peak-locking error reduction by birefringent optical diffusers. *Meas. Sci. Technol.* 29:025202

Legrand M, Nogueira J, Ventas R and Lecuona A (2012) Simultaneous assessment of peak-locking and CCD readout errors through multiple Δt strategy. *Experiments in Fluids* 53:121-135

Legrand M, Nogueira J, Jimenez R, Lecuona A and De Gregorio F (2018) Full characterization of the peak-locking error by means of orthogonal functions and application to the flow around a

helicopter fuselage model. In *19th International Symposium on the Laser and Imaging Techniques to Fluid Mechanics, Lisbon, Portugal, July 16-19*

Michaelis D, Neal DR, and Wieneke B (2016) Peak-locking reduction for particle image velocimetry. *Meas. Sci. Technol.* 27:104005

Montgomery DC, Peck EA and Vining GG (2011) *Introduction to Linear Regression Analysis*. John Wiley and Sons Inc., N.Y., 3rd edition

Nogueira J, Lecuona A, Nauri S, Legrand M and Rodriguez PA (2009) Multiple Δt strategy for particle image velocimetry (PIV) error correction, applied to a hot propulsive jet. *Meas. Sci. Technol*. 20:074001

Nogueira J, Lecuona A, Nauri S, Legrand M and Rodriguez PA (2011) Quantitative evaluation of PIV peak locking through a multiple Δt strategy: relevance to the rms component. *Experiments in Fluids* 51:785-793

Overmars EFJ, Warncke NGW, Poelma C and Westerweel J (2010) Bias errors in PIV: the pixel locking effect revisited. *In 15th International Symposium on Applications of Laser Techniques to Fluid Mechanics, Lisbon, Portugal, July 5-8*

Raffel M, Willert CE, Scarano F, Kaehler CJ, Wereley ST, and Kompenhans J (2018) *Particle Image Velocimetry– A practical guide*. Springer, 3rd edition

Roesgen T (2003) Optimal subpixel interpolation in particle image velocimetry. *Experiments in Fluids* 35:252-256

Roth GI and Katz J (2001) Five techniques for increasing the speed and accuracy of PIV interrogation. *Meas. Sci. Technol.* 12:238-245

Scharnowski S, Bross M and Kähler CJ (2019) Accurate turbulence level estimations using PIV/PTV. *Experiments in Fluids* 60:1

Timmins BH, Wilson BW, Smith BL and Vlachos PP (2012) A method for automatic estimation of instantaneous local uncertainty in particle image velocimetry measurements. *Experiments in Fluids* 53:1133-1147

Tummers MJ (1999) *Investigation of a turbulent wake in an adverse pressure gradient using laser Doppler anemometry*. PhD Thesis, Delft University Press

Westerweel J (1993) *Digital particle image velocimetry – theory and application*. PhD Thesis, Delft University Press

Westerweel J (1997) Fundamentals of digital particle image velocimetry. *Meas. Sci. Technol.* 8:1379-1392